PERGAMON

International Journal of Multiphase Flow 25 (1999) 977–1007

International Journal of Multiphase Flow

www.elsevier.com/locate/ijmulflow

The interface configuration in two-phase stratified pipe flows

Dimitri Gorelik, Neima Brauner*

Department of Fluid Mechanics and Heat Transfer, Faculty of Engineering, Tel-Aviv University, Tel Aviv 69978, Israel

Received 16 November 1998; received in revised form 1 April 1999

We would like to dedicate this paper to our dear friend and colleague, Professor Gad Hetsroni, on the occasion of his 65th birthday. We wish him continued good health and many more productive years as an international leader in the field of multi-phase flows, and a source of inspiration to us all.

Abstract

Exact analytical solution is obtained for the interface shape between two immiscible fluids and for the capillary pressure in the case of unidirectional axial laminar pipe flow. The solution is determined by three dimensionless parameters: the holdup, fluid/wall wettability angle and the Eötvös number, $Eo = \Delta\rho g \cos\alpha R^2/\sigma_{12}$. The ranges of parameter values, for which the model of flat interface ($Eo \rightarrow \infty$), or models of constant interfacial curvature can be applied, are explored. Finally, the implications to modeling of stratified flow characteristics and stability are discussed.

Keywords: Stratified flow; Interface; Curvature; Surface tension; Contact angle; Wettability

1. Introduction

Stratified flow is considered a basic flow configuration in horizontal and inclined two-phase systems of a finite density differential. Models of stratified flow are needed for predicting the flow characteristics, such as pressure drop and in-situ holdup, and are often used as a starting point in modeling flow patterns transitions.

* Corresponding author. Tel.: +972-3-640-8930; fax: +972-3-640-7334.
E-mail address: brauner@eng.tam.ac.il (N. Brauner)

PII: S0301-9322(99)00038-5

The common assumption is that the interface separating the phases is plane. This assumption is appropriate for gravity dominated systems, such as large scale gas–liquid horizontal flows under earth's gravitation. In reduced gravity systems, capillary systems or in the case of low density differential (such as oil–water systems), surface forces become important. The wetting fluid tends to climb over the tube wall resulting in a curved (convex or concave) interface. Stratified flows with curved interfaces in liquid–liquid systems have been observed both experimentally (Valle and Kvandal, 1995) and in numerical simulations (Ong et al., 1994).

A configuration of a curved interface is associated with a different contact area between the two fluids and between the fluids and the pipe wall. Depending on the physical system involved, these variations can have prominent effects on the pressure drop and transport phenomena (Brauner et al., 1995, 1998).

Once the location of the fluid interface is known, the 2D velocity profiles in steady and fully developed axial laminar flow of stratified layers, $u_1(x,y)$,$u_2(x,y)$ are obtained via analytical or numerical solutions of the following Stoke's equations (in the z direction, see Fig. 1):

$$\mu_1\left(\frac{\partial^2 u_1}{\partial x^2}+\frac{\partial^2 u_1}{\partial y^2}\right)=-\frac{\partial P_1}{\partial z}+\rho_1 g\sin\alpha \tag{1a}$$

$$\mu_2\left(\frac{\partial^2 u_2}{\partial x^2}+\frac{\partial^2 u_2}{\partial y^2}\right)=-\frac{\partial P_2}{\partial z}+\rho_2 g\sin\alpha \tag{1b}$$

The required boundary conditions follow from the no-slip condition at the pipe wall and continuity of the velocities and tangential shear stresses across the fluid's interface. For a given axial pressure drop, the solution for u_1 and u_2 can be integrated over the fluids flow cross section to yield the corresponding volumetric flow rates Q_1 and Q_2. From the practical point of view, we are interested in a solution for the pressure drop and flow geometry (interface location) for given flow rates. The inverse problem is much more complicated since the shape of fluids interface is, in fact, unknown.

In the y and x directions, the Navier–Stokes equation reduces to:

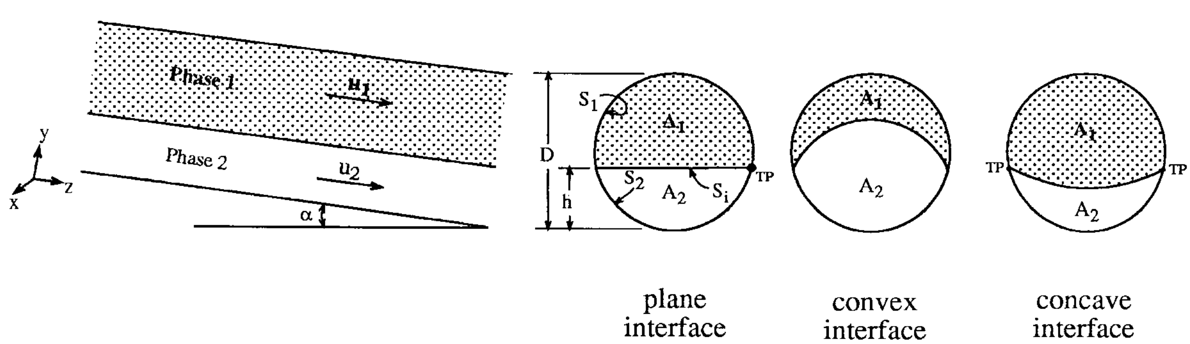

Fig. 1. Schematic description of stratified flow in a pipe.

$$-\frac{\partial P_j}{\partial y}+\rho_j\, g\cos\alpha=0;\quad j=1{,}2 \tag{2a}$$

$$\frac{\partial P_j}{\partial x}=0 \tag{2b}$$

Note that Eqs. (2a) and (2b) yield $\frac{\partial}{\partial y}(\partial P_j/\partial z)=0$ and $\frac{\partial}{\partial x}(\partial P_j/\partial z)=0$, thus, the pressure gradient in the axial direction is the same for the two fluids ($\partial P_1/\partial z=\partial P_2/\partial z=\partial P/\partial z$).

Integration of Eq. (2a) in the y direction yields a linear variation of the pressure in this direction due to the hydrostatic pressure:

$$P_1=P_{1i}-\rho_1(y-\eta)g\cos\alpha \tag{3a}$$

$$P_2=P_{2i}-\rho_2(y-\eta)g\cos\alpha \tag{3b}$$

where P_{1i}, P_{2i} are the local pressures at either side of the fluid interface, at $y=\eta(x)$. For axial, fully developed flow, the hydrodynamic stresses normal to the fluids interface vanish. In this case, the equation for the interface location evolves from the condition of equilibrium between the pressure jump across the interface and the surface tension force:

$$P_{1i}-P_{2i}=\frac{\sigma_{12}}{R_i} \tag{4}$$

where σ_{12} is the surface tension (assumed constant) between the two fluids and R_i is the local radius of the interface curvature:

$$R_i=\left\{\frac{\mathrm{d}}{\mathrm{d}x}\frac{\mathrm{d}\eta/\mathrm{d}x}{\left[1+(\mathrm{d}\eta/\mathrm{d}x)^2\right]^{1/2}}\right\}^{-1}=-\left\{\frac{\mathrm{d}}{\mathrm{d}\eta}\frac{\mathrm{d}x/\mathrm{d}\eta}{\left[1+(\mathrm{d}x/\mathrm{d}\eta)^2\right]^{1/2}}\right\}^{-1} \tag{5}$$

The interfacial curvature in the axial direction is infinite. Eq. (4) is the well-known Laplace (1806) formula that can be put (using Eqs. (2a) and (2b)) in the following form:

$$\sigma_{12}\frac{\mathrm{d}}{\mathrm{d}x}\left\{\frac{\mathrm{d}\eta/\mathrm{d}x}{\left[1+(\mathrm{d}\eta/\mathrm{d}x)^2\right]^{1/2}}\right\}-(\rho_2-\rho_1)\eta g\cos\alpha=\mathrm{const} \tag{6}$$

Eq. (6) is a non-linear differential equation for $\eta(x)$. Thus, for the flow field under consideration, the position of the fluids interface can be obtained by solving the quasi-static situation. The solution for $\eta(x)$ should comply with the wettability condition at the pipe wall and symmetry with respect to the y axis. It is also constrained by the fluids in-situ holdup available in the flow. Eq. (6) and the appropriate boundary conditions are conveniently derived by solving the variational problem of minimizing the total system (static) free energy (Bentwich, 1976).

Exact analytical solutions for the velocity profiles $u_1(x,y)$,$u_2(x,y)$ can be obtained when the fluids interface can be described by a constant curvature. In this case, the bipolar coordinate system can be applied to obtain complete analytical expressions for the velocity profiles, distribution of shear stresses along the pipe wall and fluids interface, axial pressure drop and in-situ holdup, in terms of known fluids flow rates and viscosities (Bentwich, 1964; Brauner et al., 1995, 1996a; Moalem Maron et al., 1995). The assumption of a constant curvature is trivially satisfied for a zero interfacial surface tension, where $R_i \to \infty$ in Eq. (4). In this case, the interface is plane (flat) with a zero pressure difference across the interface, and the flow geometry can be described by the thickness of the (lower) fluid layer (Fig. 1). Analytical solutions for flow with a flat interface are given in several publications (Semenov and Tochigin, 1962; Bentwich, 1964; Masliyah and Shook, 1978; Ranger and Davis, 1979; Brauner et al., 1996a).

However, in view of Eq. (6), the assumption of a constant interfacial curvature is evidently also valid when the effect of the gravitational field is negligible, as under microgravity conditions or when $\rho_2 \simeq \rho_1$. The Eötvös number $Eo = (\rho_2 - \rho_1)g \cos \alpha R^2/\sigma_{12}$ is the controlling dimensionless parameter, which evolves by non-dimensionalizing (6). The shape of the interface can be described by a constant curvature curve when $Eo \to 0$. The approach of the interface towards such configurations in cases of a finite non-vanishing Eo, depends on the values of additional system parameters, which include the fluids holdup and the fluids/wall relative wettability. In an attempt to bridge the gap between large and small Eötvös numbers, Brauner et al. (1996b) modeled the shape of the interface by a constant characteristic interfacial curvature. The characteristic curvature was found by employing the principle of minimization of the total static energy (potential and surface energies).

The range of validity of the exact solutions obtained in the two extremes of $Eo = 0$ and $Eo \to \infty$ for practical two-phase systems, as well as the approximation provided by the characteristic curvature, can be evaluated in view of a complete exact solution, which yields the interface configurations in the whole space of the system relevant parameters.

In the next section, the equations describing the interface shape are re-derived by formulating the problem a variational problem. The approach is similar to that used by Bentwich (1976), where it was demonstrated that the equations for the interface shape can be solved numerically. Here, exact analytical solutions for the interface shape are obtained for the whole range of Eötvös numbers and for various fluids holdup and fluids/wall wettability conditions. The ranges of system parameters, where the exact solutions correspond to a constant interfacial curvature, are identified. Comparison with Brauner et al. (1996b) model for the characteristic interfacial curvature shows that this model is useful for extending the range of system parameters where analytical solutions for stratified flow can be obtained.

2. The interface shape

2.1. The variational problem

The differential equation (6) for calculating the interface shape can be obtained from the variational problem of minimizing the total free energy (per unit tube length). Given the fluids holdup, the components of the free energy, that are subject to variation with changes in the interface shape, are the potential energy in the gravity field and the surface energy. Due to symmetry with respect to $x = 0$, only half of the cross-section can be considered. The potential energy (with reference to $y = 0$, see Fig. 2) is given by Gorelik (1999):

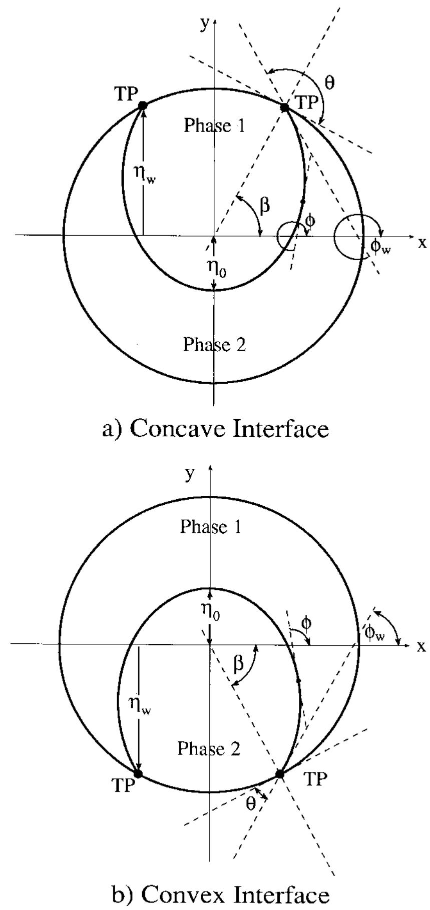

Fig. 2. Schematic description and coordinates: (a) concave interfaces (b) convex interfaces in a circular cross section.

$$E_{\mathrm{p}} = E_{\mathrm{p}_1} + E_{\mathrm{p}_2} = (\rho_2 - \rho_1) g \cos\alpha \left[\int_{\eta_{\mathrm{w}}}^{\eta_0} \eta x(\eta)\,\mathrm{d}\eta - \frac{1}{3}\left(R^2 - \eta_{\mathrm{w}}^2\right) \right] \tag{7}$$

The surface free energy, E_{s} consists of the interfacial energy, $E_{\mathrm{s}_{12}}$ (due to the surface tension between the two fluids, σ_{12}) and the wall energy, $E_{\mathrm{s}_{\mathrm{w}}} = E_{\mathrm{s}_{1\mathrm{w}}} + E_{\mathrm{s}_{2\mathrm{w}}}$ (due to the wall/fluids surface tension coefficients, $\sigma_{1\mathrm{w}}$ and $\sigma_{2\mathrm{w}}$). These surface energies are given by:

$$E_{\mathrm{s}_{12}} = \sigma_{12} \left| \int_{\eta_{\mathrm{w}}}^{\eta_0} \left[1 + x_\eta^2 \right]^{1/2} \mathrm{d}\eta \right| \tag{8a}$$

$$E_{\mathrm{s}_{\mathrm{w}}} = (\sigma_{2\mathrm{w}} - \sigma_{1\mathrm{w}}) R \sin^{-1}\left(\frac{\eta_{\mathrm{w}}}{R}\right) + \frac{\pi R}{2}(\sigma_{1\mathrm{w}} + \sigma_{2\mathrm{w}}) \tag{8b}$$

where $x_\eta = \mathrm{d}x/\mathrm{d}\eta$. Note that since $E_{\mathrm{s}_{12}} > 0$, the rhs of Eq. (8a) should yield a positive value both for $\eta_0 > \eta_{\mathrm{w}}$ and $\eta_{\mathrm{w}} > \eta_0$. For a given holdup, the value of the total energy, $E = E_{\mathrm{p}} + E_{\mathrm{s}}$

depends on the shape $x(\eta)$ of the interface. The equilibrium shape will be that which minimizes E, subject to a constraint of a constant fluids holdup:

$$\varepsilon_1 = \frac{A_1}{A} = \frac{\tilde{\eta}_w}{\pi}\sqrt{1-\tilde{\eta}_w^2} - \frac{1}{\pi}\sin^{-1}\tilde{\eta}_w + \frac{2}{\pi}\int_{\tilde{\eta}_w}^{\tilde{\eta}_0} \tilde{\eta}\tilde{x}_{\tilde{\eta}}\, d\tilde{\eta} + \frac{1}{2} = \text{constant} \tag{9}$$

where $\sim$ denotes values normalized by R.

The problem is solved by standard variational calculus. The functional that is being minimized is $G = E + \lambda A_1$, where λ is a Lagrangian multiplier. The condition that δG should be zero for all possible variations in η (including η_w and η_0) yields the Euler–Lagrange equation for the problem at hand:

$$\eta(\rho_2 - \rho_1)g\cos\alpha \mp \sigma_{12}\frac{d}{d\eta}\frac{x_\eta}{\left(1+x_\eta^2\right)^{1/2}} + \lambda = 0 \tag{10}$$

where the upper sign in Eq. (10) applies for $\eta_w > \eta_0$ (concave interface).

For arbitrary η_0 and η_w the natural boundary conditions evolve. For convenience, the angles ϕ and β are first defined (see Fig. 2):

$$\text{ctg}\,\phi = \frac{dx}{d\eta}; \quad \phi|_{x=0} = \phi_0; \quad \phi|_{x=x_w} = \phi_w \tag{11a}$$

$$\cos\beta = \frac{x_w}{R}; \quad \sin\beta = \frac{\eta_w}{R}; \quad -\frac{\pi}{2} \le \beta \le \frac{\pi}{2} \tag{11b}$$

In terms of ϕ and β, the natural boundary conditions obtained are:

$$\text{at } x = 0; \quad \frac{d\eta}{dx} = 0 \text{ or } \phi|_{x=0} = \phi_0 = \pi \tag{12a}$$

$$\text{at } x = x_w; \quad tg^{-1}\left(\frac{d\eta}{dx}\right) = \phi_w = \frac{\pi}{2} + \beta + \theta; \quad 0 \le \phi_w \le 2\pi \tag{12b}$$

where θ is the fluids/wall wettability angle, which is related to the surface free energies by Young equation:

$$\cos\theta = \frac{\sigma_{2w} - \sigma_{1w}}{\sigma_{12}}; \quad 0 \le \theta \le \pi \tag{13}$$

Boundary condition (12a) yields solutions for $\eta(x)$ which are symmetrical with respect to the y axis. At the triple point (TP, where the interface is in contact with the wall), condition (12b) imposes the fluids/wall wettability condition (see Fig. 2).

Eq. (10) is the Laplace equation applicable to the particular problem. The fact that it is identical to Eq. (6) implies that the formulation of a variational problem that minimizes the system potential and surface energies, is consistent with the hydrodynamic equations for unidirectional and fully developed axial flow. Hence, no other energies (such as the fluids kinetic energies) should have been included in the analysis.

The λ term in Eq. (10) (which replaces the constant in Eq. (6)), evolves from the constraint on the phases volume. Physically, it expresses the fact that for enclosed fluids, the local pressure difference across the interface can be determined in terms of the hydrostatic pressure up to a level of a priori unknown constant. Mathematically, it represents the magnitude of a priori unknown surface tension force at some reference point (say $\eta = 0$). The value of this constant as function of the system parameters is obtained as part of the solution of the problem.

2.2. Mathematical solution

Eq. (10) is a nonlinear differential equation for $x(\eta)$. This form is convenient since $x(\eta)$ is single valued ($\eta(x)$ may be double valued) and may have several inflection points. In terms of dimensionless variables, $\tilde{x} = x/R, \tilde{\eta} = \eta/R$, Eq. (10) reads:

$$\tilde{\eta} + \Lambda - \frac{a_v^2}{2}\frac{\mathrm{d}}{\mathrm{d}\tilde{y}}\cos\phi = 0 \tag{14a}$$

where

$$a_v^2 = \frac{2\sigma_{12}}{\Delta\rho g\cos\alpha R^2} = \frac{2}{E_0}; \qquad \Lambda = \frac{\lambda}{\Delta\rho g\cos\alpha R^2} \tag{14b}$$

Integration of Eq. (14) with respect to $\tilde{y}$ yields an explicit relation between local values of $\tilde{\eta}$ and ϕ:

$$\tilde{\eta} = \pm a_v\sqrt{A + \cos\phi} - \Lambda \tag{15}$$

where A is an unknown integration constant. Differentiating Eq. (15) with respect to $\tilde{x}$ yields:

$$\mathrm{d}\tilde{x} = \mp a_v \frac{\cos\phi}{\left[A + \cos\phi\right]^{1/2}}\,\mathrm{d}\phi \tag{16}$$

The choice of an appropriate sign in Eqs. (15) and (16) depends on the range of variation of ϕ along the interface curve. It should be carefully examined when passing through inflection points. When the lighter phase is the more wetting phase, $0<\theta<\pi/2$ and $0\le\phi_w\le\pi$, the upper sign applies, whereas the lower sign corresponds to $\pi/2<\theta\le\pi$ and $\pi<\phi_w\le 2\pi$ (the heavier fluid is the wetting phase). Other choices of sign in Eqs. (15) and (16) yield unphysical discontinuous solutions for $\eta(x)$ (Gorelik, 1999).

Integration of Eq. (16) using boundary condition (12) and straightforward manipulations yields a solution for $\tilde{x}(\phi)$:

$$\tilde{x} = \pm \frac{a_v k}{\sqrt{2}} \left\{ \left(\frac{2}{k^2} - 1 \right) \left[F_1\left(k, \frac{\pi}{2}\right) - F_1\left(k, \frac{\pi - \phi}{2}\right) \right] - \frac{2}{k^2} \left[F_2\left(k, \frac{\pi}{2}\right) - F_2\left(k, \frac{\pi - \phi}{2}\right) \right] \right\} \tag{17}$$

where $k = \sqrt{\frac{2}{A+1}}$. The functions $F_1(k,\phi),F_2(k,\phi)$ represent elliptical integrals of the first and second kind respectively and are given by series of the trigonometric functions (Grandsteyn and Rezhik, 1980). Note that $F_1(k,\pi/2)$ is the complete elliptical integral, usually denoted by $F_1(k)$. Tabulated values of elliptical integrals can be found in Abramowitz and Stegun (1964). The solution is completed when the constants A (or k) and Λ are determined. Substituting boundary condition (12b) in (17) yields:

$$\pm \frac{a_v k}{\sqrt{2}} \left\{ \left(\frac{2}{k^2} - 1 \right) \left[F_1\left(k, \frac{\pi}{2}\right) - F_1\left(k, \frac{\pi/2 - \beta - \theta}{2}\right) \right] - \frac{2}{k^2} \left[F_2\left(k, \frac{\phi}{2}\right) - F_2\left(k, \frac{\pi/2 - \beta - \theta}{2}\right) \right] \right\} - \cos\beta = 0 \tag{18}$$

It is to be noted that the minimal value of A is 1 and $A \rightarrow 1 (k \rightarrow 1)$ as the interface approaches a plane configuration. Its value increases with increasing a_v. Thus, given a_v,θ and β, Eq. (18) represents a non-linear algebraic equation in a single unknown, k. Once a solution for k is obtained, the complete interface shape is defined by Eqs. (15) and (17). The value of Λ can be calculated by applying Eq. (15) at the triple point where $\tilde{\eta} = \sin\beta$ and $\phi = \phi_w$, whereby:

$$\Lambda = \pm a_v \sqrt{A + \cos\phi_w} - \sin\beta \tag{19}$$

The corresponding fluids holdup is obtained by Eq. (9), which in terms of β reads:

$$\varepsilon_1 = \frac{1}{\pi} \left[\frac{1}{2} \sin 2\beta - \beta + \frac{\pi}{2} + 2 \int_{\sin\beta}^{\tilde{\eta}_0} \tilde{\eta} \tilde{x}_{\tilde{\eta}} \, d\tilde{\eta} \right] \tag{20}$$

One should realize, however, that β is actually a priori unknown. The set of known parameters includes a_v (or the Eötvös number), the wettability angle, θ and the fluids holdup ε_1. From the practical point of view, it is of interest to obtain solutions in terms of these three parameters. This requires an iterative solution, whereby a search for a value of β that meets a prescribed value for the fluids holdup is carried out. The search is facilitated by deriving an explicit expression for Λ in terms of the holdup. Integrating Eq. (14a) with respect to $\tilde{y}$ (after multiplying it by $x_{\tilde{\eta}}$) and employing the constraint on the fluids holdup (20) yields:

$$\Lambda = \frac{1}{2\cos\beta} \left[\pi\varepsilon_1 + \beta - \frac{\pi}{2} - \frac{1}{2}\sin 2\beta - a_v^2 \cos(\theta + \beta) \right] \tag{21}$$

The solution is carried out by using Eqs. (18) and (19) for a prescribed β to obtain A and Λ

and then iterating on β which satisfies Eq. (21). Note that, the use of Eq. (21) instead of Eq. (20) as a constraint on the fluids holdup, avoids the integration required in rhs of Eq. (20).

2.3. Solution for $a_v \to \infty$

The limit of $a_v \to \infty$ ($Eo \to 0$) corresponds to systems where gravity can be ignored compared to surface forces. In this limit, the solution of Eq. (10) with boundary conditions (12a) and (12b) simplifies and is given by the following equations:

$$\tilde{x} = -\frac{a_v^2}{2\Lambda}\sin\phi \tag{22}$$

$$\Lambda\tilde{y} = -\frac{a_v^2}{2\Lambda}\cos\phi - C \tag{23}$$

where

$$\Lambda = -\frac{a_v^2}{2}\frac{\sin\phi_{\mathrm{w}}}{\cos\beta_\infty}$$

$$C = -\frac{a_v^2}{2}\left[\cos\phi_{\mathrm{w}} + \sin\phi_{\mathrm{w}} tg\beta_\infty\right] \tag{24}$$

In the limit of very large capillary numbers, the curvature of the interface is constant and (for a given holdup) is determined by the wettability angle. The constant curvature provides a simple description of the two-phase geometry and enables obtaining explicit expressions for the holdup and the length of the interface. In terms of ϕ_{w} and β_∞, these are given by:

$$\varepsilon_2 = \frac{1}{\pi}\left\{\left[\frac{\pi}{2} + \beta_\infty + \frac{1}{2}\sin 2\beta_\infty\right] - \frac{\cos^2\beta_\infty}{\sin^2\phi_{\mathrm{w}}}\left[\phi_{\mathrm{w}} - \pi - \frac{1}{2}\sin 2\phi_{\mathrm{w}}\right]\right\}; \quad \phi_{\mathrm{w}} \neq 0,\pi$$

$$\varepsilon_2 = \frac{1}{\pi}\left[\frac{\pi}{2} + \beta_\infty + \frac{1}{2}\sin 2\beta_\infty\right]; \quad \phi_{\mathrm{w}} = 0,\pi \tag{25}$$

and

$$\tilde{S}_i = 2\left|\int_{\tilde{\eta}_{\mathrm{w}}}^{\tilde{\eta}_0}\left(1 + \tilde{x}_{\tilde{\eta}}^2\right)^{1/2}\mathrm{d}\tilde{\eta}\right| = \frac{2(\pi - \phi_{\mathrm{w}})\cos\beta_\infty}{\sin\phi_{\mathrm{w}}}; \quad \phi_{\mathrm{w}} \neq 0,\pi$$

$$\tilde{S}_i = 2\cos\beta_\infty; \quad \phi_{\mathrm{w}} = 0,\pi \tag{26}$$

where S_i is the interface length ($\tilde{S}_i = S_i/R$) and $\phi_{\mathrm{w}} = \pi/2 + \beta_\infty + \theta$.

2.4. Results

The mathematical solution yields analytical equations for calculating the shape of the interface, $\tilde{\eta}(\tilde{x})$ and Λ. These are obtained in terms of three dimensionless parameters: the Eötvös number (or a_v), the fluid/wall wettability angle, θ and the fluids holdup. The function $\tilde{\eta}(\tilde{x})$ determines the geometry of the fluids distribution in the pipe cross section and contact with the pipe wall, whereas Λ is required for calculation of the pressure distribution.

The first important point to realize is, that in a pipe, the interface shape varies with the fluids holdup. This is demonstrated in Fig. 3 where the solutions for $\tilde{\eta}(x)$ are given for a constant Eötvös number and different fluids holdup. The case of $\theta = 90°$ (Fig. 3a) corresponds to equal wettability of the two fluids. In this case, the interface is concave for relatively low holdup of the upper phase, $\varepsilon_1 < 0.5$ and convex for $\varepsilon_1 > 0.5$. For the particular case of $\varepsilon_1 = \varepsilon_{1p} = 0.5$, the interface is plane, since this configuration satisfies the wettability condition

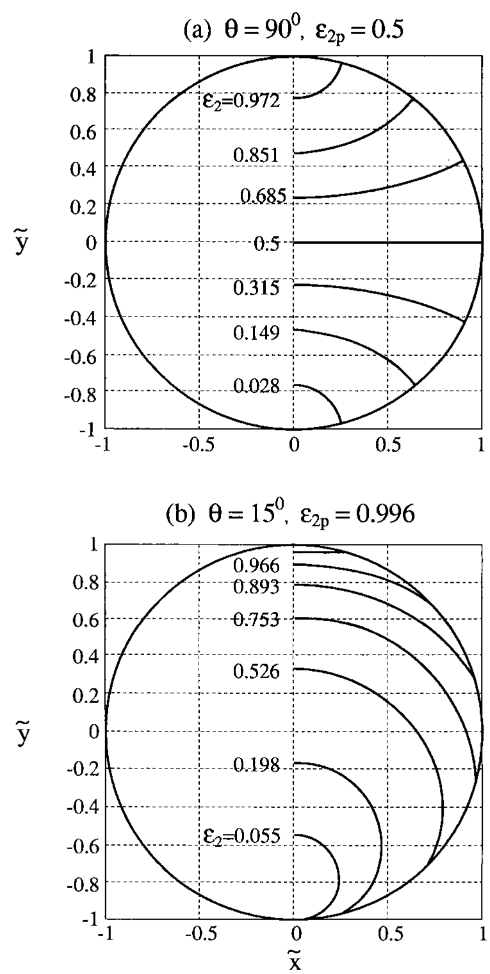

Fig. 3. Interface configurations for $a_v = 2$ ($Eo = 1$): effect of holdup for $\theta = 90°$ and $\theta = 15°$.

at the solid wall. When the upper phase is the more wetting phase ($\theta < 90°$),ε_{1p} decreases, as shown in Fig. 3b (for $\theta = 15°, \varepsilon_{1p} \simeq 0.004$).

Note that the symmetrical case of $\theta = 165°$ (the lower liquid is the wetting phase) is obtained by rotating Fig. 3b by 180° around the pipe center and replacing values of ε_1 by ε_2. Generally, the interface shapes in a system (B) where $\frac{\pi}{2} < \theta \leq \pi$ (the lower fluid is the more wetting phase) can be deduced from results obtained for symmetrical configurations corresponding to $0 \leq \theta \leq \frac{\pi}{2}$ (system A), using the following rule:

When

$$(a_v)_A = (a_v)_B$$

$$(\theta)_A = \pi + (\theta)_B$$

$$(\varepsilon_1)_A = (\varepsilon_2)_B \tag{27a}$$

then

$$(\tilde{\eta})_A = -(\tilde{\eta})_B \tag{27b}$$

The value of ε_{1p} approaches zero as $\theta \rightarrow 0$ and the interface is convex independently of the fluids holdup ($\varepsilon_{2p} \rightarrow 0$ as $\theta \rightarrow \pi$ and the interface is always concave). However, for partial wettability ($\theta \neq 0, \pi$) there is a particular value of holdup, ε_{1p}, where adhesion forces to the wall are just balanced at the triple point and the system behaves as pseudo gravitational — the interface is plane independently of the Eötvös number. For $\varepsilon_1 \neq \varepsilon_{1p}$ the interface curvature increases with increasing a_v (reducing Eo).

The dependence of the interface shape on the fluids holdup is a basic difference between pipe flow and channel flow. In a rectangular cross section, the interfacial shape is invariant with the fluids holdup, except for low holdup of one of the phases, where the interfacial shape may be constrained by the presence of the upper, or lower wall. Otherwise, the holdup affects only the average interface level. For $\theta < \pi/2$, the interface is always convex, and it is concave for $\theta > 90°$. For $\theta = 90°$ the system is pseudo gravitational independent of the Eötvös number and holdup. The solution for the interface shape in a rectangular cross section is given in Appendix A.

One of the most important characteristic of the interface shape is the location of its contact with the tube wall (the TP point), described by the value of β (see Fig. 2). The value of β determines the portion of the tube perimeter which is wetted by each of the fluids and has an obvious effect on the pressure drop and wall/fluids transport phenomena. Note that for $\beta \rightarrow 90°$, the wall is entirely wetted by the lower phase, whereas $\beta \rightarrow -90°$ corresponds to configurations where the wall is wetted only by the upper phase.

The effect of the wettability angle on the variation of β with the holdup and the capillary number can be studied in view of Fig. 4. The values of β corresponding to a plane interface are given by the curve for $a_v = 0$, which is applicable when surface forces vanish. The other extreme of no gravity force is described by the curve of $a_v \rightarrow \infty$. Fig. 4a is for ideal wettability of the upper phase ($\theta = 0°$). For this case $\varepsilon_{1p} = 0$ and the interface is convex for any non-vanishing value of the capillary number ($\beta < \beta_0 = \beta_{(a_v=0)}$ over the entire range of holdup). The

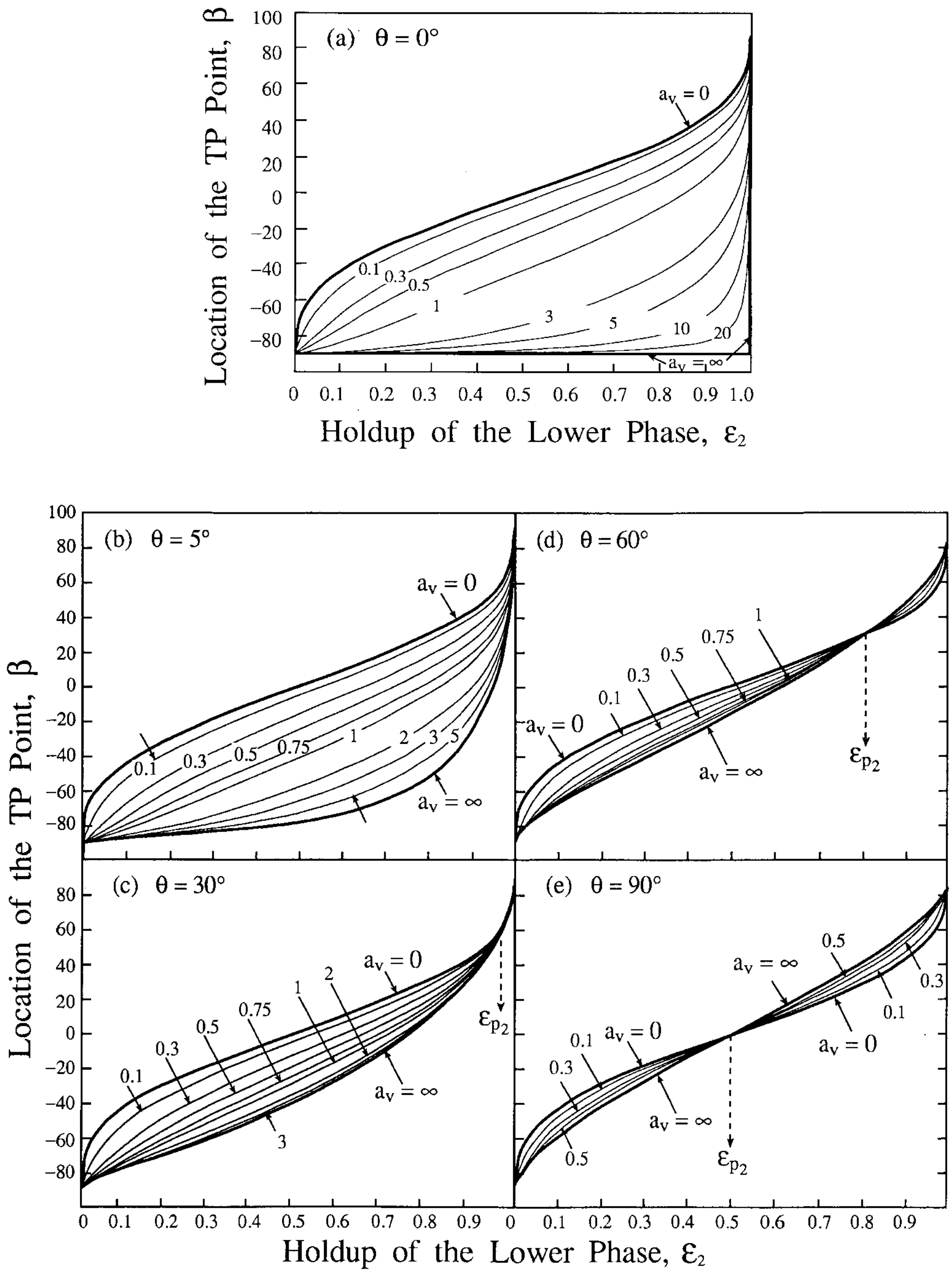

Fig. 4. The fluids contact with the wall: variation of β with the holdup for various capillary numbers and wettability angles.

figure shows that the values of β deviate from those predicted by a plane interface already for a small capillary number, such as $a_v = 0.1$. Note that horizontal flow of air and water in a 1 in. tube corresponds to $a_v = 0.3$ and it increases with reducing the density difference (as in oil water systems), reducing the tube diameter, or reducing the gravity field by inclining the tube to the horizontal.

Fig. 4a and b show that for a given holdup, β values vary over a considerable range with changing a_v. With increasing a_v, the upper wetting fluid wets a larger portion of the tube perimeter. For sufficiently high capillary number, the variation of β with the holdup approaches a uniform curve obtained by the solution for $a_v \to \infty$. In cases of almost ideal wettability of the upper phase, the curve of $a_v \to \infty$ provides a lower bound on the value of β. For $\theta = 5^\circ$, this lower bound is greater than -90°, in particular for high holdup of the lower (non-wetting) fluid. For low holdup of the lower (non-wetting) fluid, $\beta \to -90^\circ$, indicating that the lower fluid is almost encapsulated by the upper wetting phase. The value of -90° is approached asymptomatically for $\theta = 0$ and large a_v (Fig. 4a), whereby the wetting fluid completely encapsulates the lower fluid and a configuration of a fully eccentric core-annular configuration is formed irrespective of the holdup.

The variation of β with the capillary number is moderated with reducing the difference in the wetting tendency of the two fluids. This trend is clearly seen in Fig. 4a–e. As $\theta \to \pi/2$, the difference between the value of β_0 (corresponding to $a_v = 0$, flat interface) and β_∞ (for $a_v \to \infty$) diminishes. Fig. 4c–e show that all curves of $\beta(\varepsilon_2, a_v)$ intersect at $\varepsilon_2 = \varepsilon_{2\mathrm{p}}$, where the interface is plane irrespective of the capillary number. In systems of $\theta < \pi/2$, the interface is convex for $\varepsilon_2 < \varepsilon_{2\mathrm{p}}$ and β values are bounded below by β_∞ and above by β_0. The bounds are reversed for $\varepsilon_2 > \varepsilon_{2\mathrm{p}}$, where the interface is concave and the more wetting fluid wets a smaller portion of the tube perimeter than that under gravity dominated conditions ($a_v = 0$). Inspection of Fig. 4a–e indicates that, with increasing a_v, the approach of the β values to β_∞ is faster as $\theta \to \pi/2$.

The approach of the interface shape to the solutions obtained for $a_v = 0$ or $a_v \to \infty$, and the range of parameters where the solutions in either of these extremes can be used to describe the phases geometry, are further studied in view of Figs. 5–8. These figures show the absolute and relative deviation in the wetted perimeter of the lower phase, and the relative deviation in the length of the interface when the interface is modeled either as planar (Figs. 5 and 6), or by the constant curvature predicted by the $a_v \to \infty$ solution (Figs. 7 and 8). Obviously, the approximation provided by a model of a plane interface deteriorates as a_v increases, whereas the approximation provided by the solution of $a_v \to \infty$ deteriorates with reducing a_v.

Considering an error of $\approx$10–15% as acceptable, Figs. 5 and 6 show that when a model of flat interface is used, this error level is exceeded already for $a_v \approx 0.2$. Even with a small a_v, for small holdups of the non-wetting (lower) phase, the relative error in its wetted perimeter exceeds 100%. The relative error escalates with increasing the capillary number. The large relative errors for low ε_2 result from the tendency of the wetting phase to ecapulate small amounts of the non-wetting phase and to diminish its contact with the wall already at relatively small capillary numbers.

Inspection of the deviations associated with the model of $a_v \to \infty (Eo \to 0)$ in Figs. 7 and 8 indicates that this model provides a good approximation for $a_v > 5$. The predictions improve as the holdup of the less wetting phase decreases. Since the errors are zero also for $\varepsilon_2 = 1$ (single phase) the largest deviations are in the range of $0.5 < \varepsilon_2 < 0.85$.

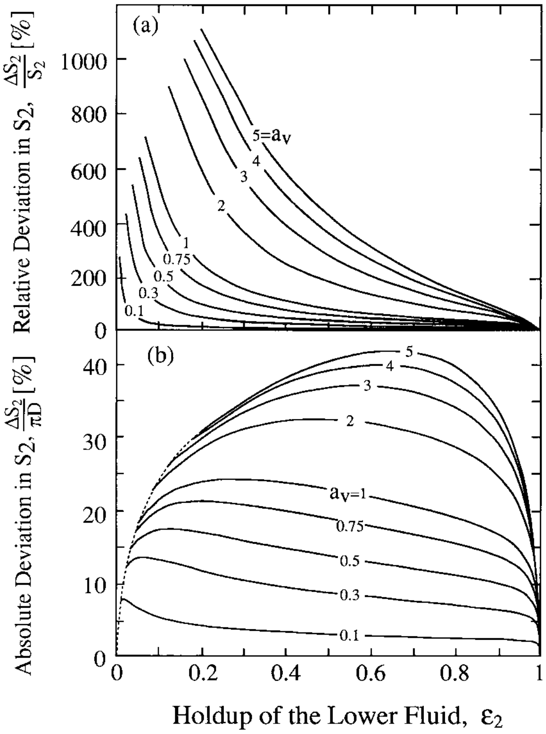

Fig. 5. The deviation in the lower phase wetting perimeter when a model of a plane interface is used ($\theta = 5°$).

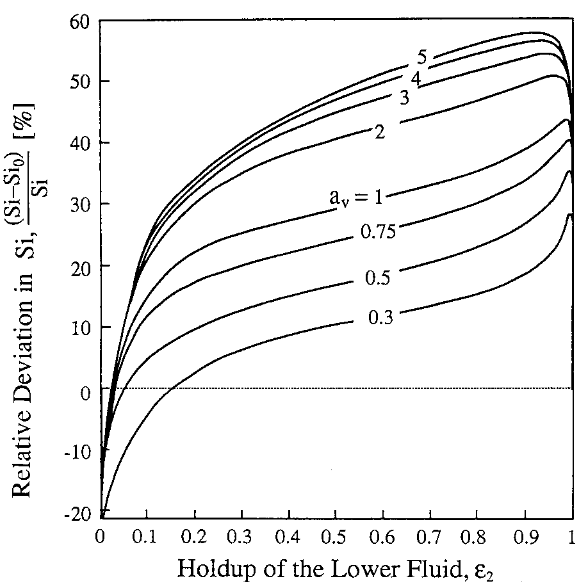

Fig. 6. The deviation in the interface length when a model of a plane interface is used ($\theta = 5°$).

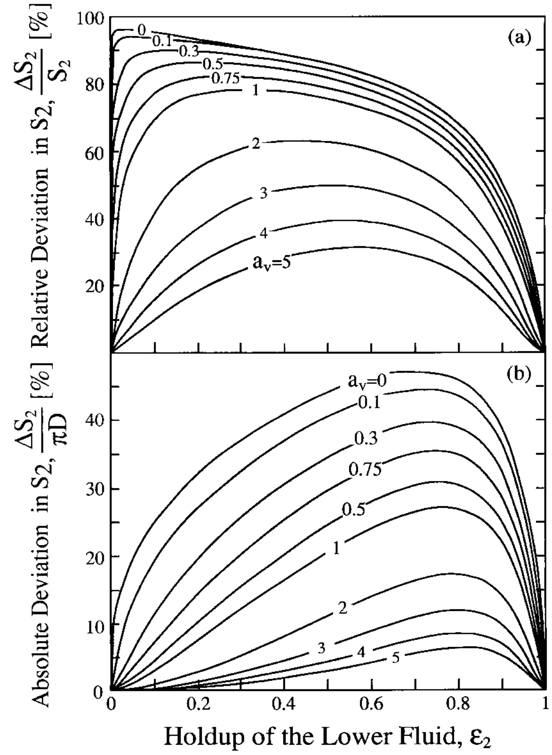

Fig. 7. The deviation in the lower phase wetting perimeter when the model for $a_v \to \infty$ ($Eo = 0$) is used ($\theta = 5°$).

In view of Figs. 5–8, there is a considerable range of capillary numbers where neither the model of flat interface ($a_v \to 0$) nor the model of the $a_v \to \infty$ constant curvature, correctly describes the phases geometry. Although this range decreases as the fluids/wall wetting tendency becomes similar ($\theta \to \pi/2$), the parameters space where the exact solution should be applied does not diminishes to zero.

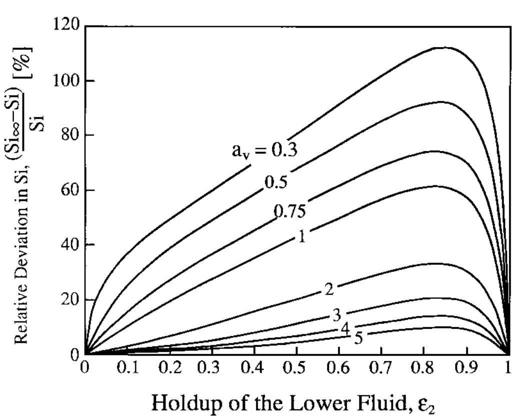

Fig. 8. The deviation in the interface length when the model of $a_v \to \infty$ ($Eo = 0$) is used ($\theta = 5°$).

Another important outcome of the solution is the variation of Λ with the parameters of the solution. The value of Λ is required for calculating the pressure distribution in the cross section and the average pressure force acting on each of the fluids cross section.

The physical significance of the parameter Λ can be understood by examining its value in the limits of $a_v \rightarrow 0$ or $a_v \rightarrow \infty$. When surface tension forces are ignored ($a_v = 0$), the interface is plane and is given by $\tilde{\eta} = \tilde{h} - 1$, ($h$ is measured from the tube bottom) and Eq. (10) yields:

$$\Lambda_0 = \Lambda|_{a_v=0} = 1 - \tilde{h} = \frac{1}{2\cos\beta_0}\left[\sin\beta_0 + \beta_0 + \pi\varepsilon_1\right] = \sin\beta_0 \tag{28}$$

In this case, Λ is a constant dimensionless pressure along the interface due to the gravity field. In the other extreme of $a_v \rightarrow \infty$ Eqs. (10), (12) and (14) yield:

$$\Lambda_\infty = \Lambda|_{a_v \rightarrow \infty} = -\frac{a_v^2}{2}\frac{\cos(\theta + \beta_\infty)}{\cos\beta_\infty} \tag{29}$$

In this case, Λ_∞ represents a constant (dimensionless) capillary pressure jump along the interface due to the constant curvature. Comparison of Eqs. (28) and (29) with Eq. (21) shows that due to the fact that $\beta_0 \neq \beta_\infty$ the value of Λ cannot be represented as a superposition of the above two asymptotic values (as is permitted in a rectangular cross section, see (A10) to (A13) in Appendix A). However, in view of Eq. (10) (or Eq. (14)) the value of Λ for any a_v can be represented by a superposition of Λ_0 and the contribution of the surface tension force due to the interfacial curvature at the point $\tilde{\eta} = \tilde{h} - 1$ (where the interface level is identical to that of a plane interface). In view of the above interpretation of Λ and its relation to the interfacial curvature, R_i^{-1} at $\tilde{\eta} = \tilde{h} - 1$, the following scaling is used to represent the net effect of surface forces (the capillary pressure) on the value of Λ:

$$\tilde{\Lambda} = \frac{\tilde{R}_i^{-1}(\tilde{\eta} = \tilde{h} - 1)}{\tilde{R}_i^{-1}(a_v \rightarrow \infty)} = \frac{2\cos\beta_\infty}{a_v^2\cos(\beta_\infty + \theta)}[\Lambda - \Lambda_0] \tag{30}$$

Note that for a specific holdup, the values of Λ_0 and β_∞ (see Section 2.3) can be easily obtained. The variation of the rhs of Eq. (30) with the capillary number, for constant wettability angle θ and specified values of the holdup, are shown in Fig. 9. Obviously for $a_v \rightarrow 0, \Lambda \rightarrow \Lambda_0$, and therefore, all curves go to $\tilde{\Lambda} = 0$. In the other extreme of $a_v \rightarrow \infty, \tilde{\Lambda} \rightarrow 1$. The value of $\tilde{\Lambda} = 1$ is also approached for finite a_v, when the holdup in the system approaches $\varepsilon_{2\mathrm{p}}$. As discussed with reference to Figs. 3 and 4, when $\varepsilon_2 = \varepsilon_{2\mathrm{p}}$ the interface is plane irrespective of the a_v, and $\tilde{R}_i^{-1} \equiv 0$. Hence, for $\varepsilon_2 = \varepsilon_{2\mathrm{p}}, \tilde{\Lambda} = 1$ for all a_v values. Consequently, the variation of $\tilde{\Lambda}$ with the holdup (or β) exhibits a non-monotonous and complex variation, as is further demonstrated in Fig. 10.

Another point which deserves attention is that the values of $\tilde{\Lambda}$ are not bounded by those predicted via the $a_v \rightarrow \infty$ model. As is shown in Figs. 9 and 10, $\tilde{\Lambda}$ overshoots the value of 1, implying that the local interface curvature for a finite a_v can exceed the constant curvature that is obtained in the limit of $a_v \rightarrow \infty$, thereby increasing the capillary pressure. The overshoot in $\tilde{\Lambda}$ is moderated and eventually vanishes, as $\theta \rightarrow \pi/2$.

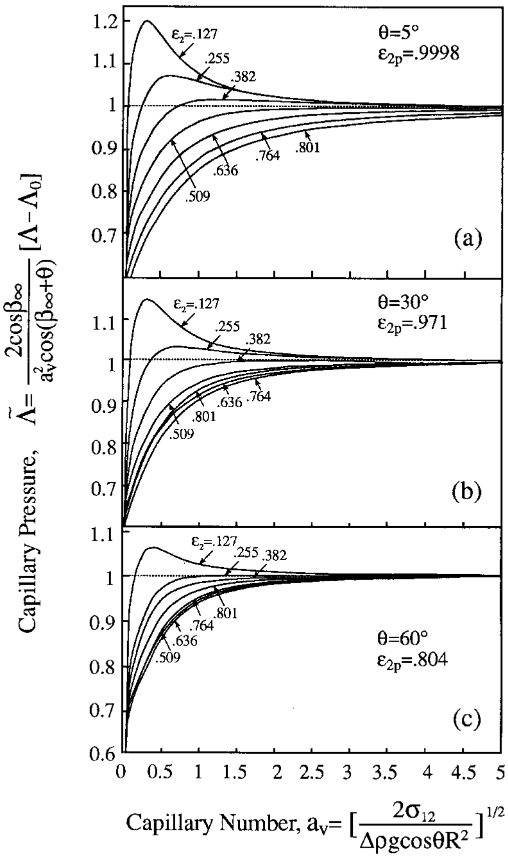

Fig. 9. Variation of the capillary pressure with a_v for different holdups and $\theta = 5°, 30°, 60°$.

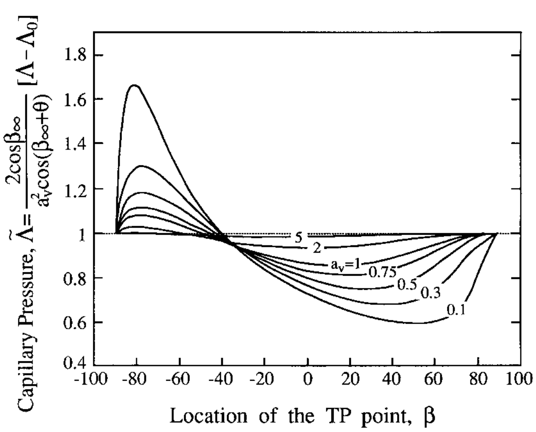

Fig. 10. Variation of the capillary pressure with β for $\theta = 5°$ and different values of a_v.

3. Comparison with Brauner et al. (1996b) model

Analytical solutions of the Stokes equations for stratified flows in pipes can be obtained, if the fluids interface can be described by a curve of a constant curvature. In order to obtain the appropriate characteristic interfacial curvature, Brauner et al. (1996b) formulated the variational problem of minimizing the sum of the system potential and surface energies with approximate configurations that are described by a priori unknown constant curvature. The curvature and the location of the TP are subject to variations which are constrained by a prescribed fluids holdup.

Taking a configuration of flat interface as a reference, the expression obtained for the system free energy, in terms of the variables used in this study (ϕ^*,ϕ and α in Brauner et al. (1996b) are replaced by ϕ_w,$\beta+\pi/2$ and $(\pi-\theta)$, respectively) reads:

$$\tilde{E}=\frac{E_s+E_p}{R^3(\rho_2-\rho_1)g\cos\alpha}=\left\{\frac{\cos^3\beta}{\sin^2\phi_w}(\operatorname{ctg}\phi_w+\operatorname{ctg}\beta)\left[\pi-\phi_w+\frac{1}{2}\sin 2\phi_w+\frac{2}{3}\cos^3\beta_0\right]\right.$$
$$\left.+a_v^2\left[\cos\phi_0\frac{(\pi-\phi_w)}{\sin\phi_w}-\cos\beta_0+\cos\theta(\beta-\beta_0)\right]\right\} \tag{31}$$

Given a_v,θ and ε_2, the equilibrium interface shape is determined by β and ϕ_w, which correspond to a minimum of $\tilde{E}$, subject to the constraint:

$$\varepsilon_2=\frac{1}{\pi}\left\{\beta+\pi/2+\frac{1}{2}\sin(2\beta)-\frac{\cos^2\beta}{\sin^2\phi_w}\left[\phi_w-\pi-\frac{1}{2}\sin(\phi_w)\right]\right\};\quad \phi_w\neq\pi$$
$$\varepsilon_2=\frac{1}{\pi}\left(\beta+\frac{\pi}{2}+\frac{1}{2}\sin 2\beta\right);\quad \phi_w=\pi \tag{32}$$

Note that in the exact solution for the interface shape ϕ_w is determined by β and the wettability angle (see Fig. 2 and Eq. (12b)). In the approximate solution, b.c Eq. (12b) is relaxed, and the solution obtained for ϕ_w only approximately satisfies the wettability condition. However, in the extremes of $a_v=0$ or $a_v\to\infty$ (where also the exact interfacial shapes correspond to a constant curvature) the approximate and exact solution coincide, whereby:

$$\phi_w=\pi;\quad \text{for}\ \ a_v=0, Eo\to\infty$$
$$\phi_w=\theta+\beta+\pi/2;\quad \text{for}\ \ a_v\to\infty, Eo\to\infty \tag{33}$$

Fig. 11 shows a typical comparison between the interface configurations of the exact solution and that described by the constant characteristic curvature. The approximate solution closely follows the exact solution in describing the effect of the holdup on the curving of the interface. Fig. 11b summaries results for β obtained with various wettability angles and shows that the comparison improve as $\theta\to\pi/2$. The largest deviations are for $\theta=5°$ (or $\theta=175°$). However, for $\theta=45°$ (or 135°) the difference between the two solutions is already un-noticeable.

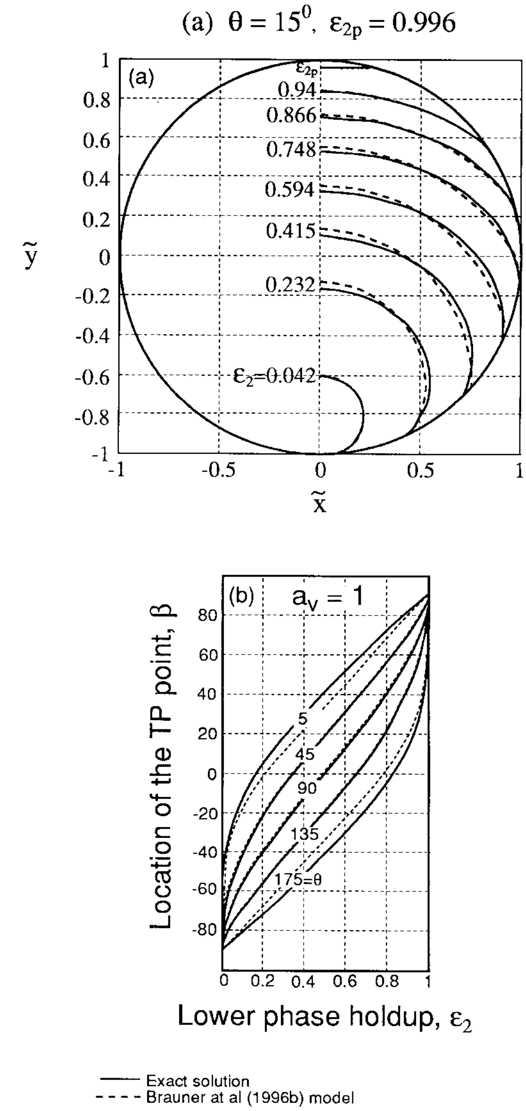

Fig. 11. Comparison of the characteristic curvature model with the exact solution, $a_v = 1$: (a) curves of $\tilde{\eta}(x)$ for $\theta = 15°$, (b) value of β vs. ε_2 for various θ.

The relative and absolute deviations in the wetted perimeter of the lower phase which are associated with the approximate solution are shown in Figs. 12 and 13. The absolute deviation is bounded by 4.5%, which is approached for $a_v \simeq 0.5$–1 and $\theta = 5°$. In this parameters range the relative deviation is maximal and may reach 30%, but only for small holdup of the lower (non-wetting) phase, where $\beta \rightarrow 0$ and the wetted perimeter of the lower phase diminishes to a very small length. Comparison with Figs. 5 and 7 shows that in this region, the relative deviations of the other approximate models (either a plane interface model or the high

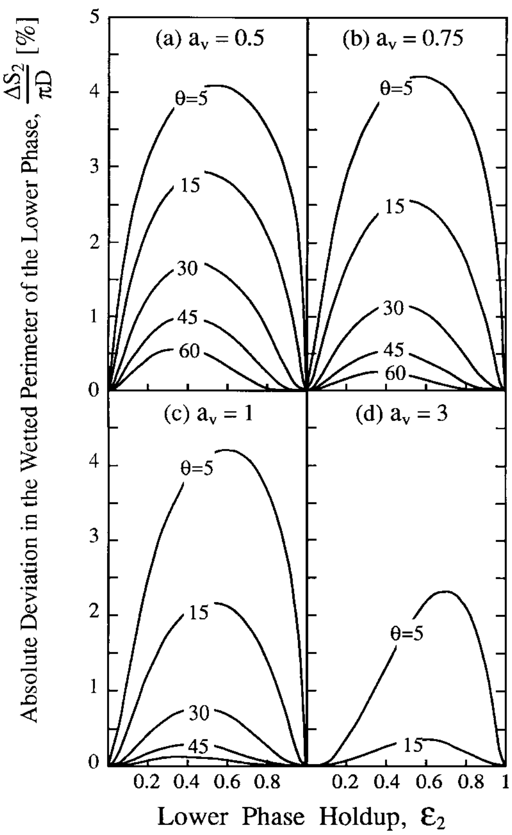

Fig. 12. The absolute deviations in the values of lower phase wetted perimeter associated with the model of constant characteristic curvature (Brauner et al., 1996b).

capillary number model) escalates to extremely high values (larger than 1000%). The parameters range presented in Figs. 12 and 13 is associated with the maximal errors. The absolute errors and relative errors decrease when $a_v > 1$ or $a_v < 0.5$ and when $\theta \to \pi/2$. Note that for $a_v \geq 1$ and $\theta \geq 45°$ the deviations of the approximate solution are less than 1% The relative deviations associated with the wetted perimeter of the upper phase (which is the more wetting phase) are even lower.

The above trends are also indicated by the error associated with the interface length (Fig. 14). Note that in the characteristic curvature model the interface length is given by a simple analytical expression (the same as Eq. (26)). Fig. 14a (for $a_v = 0.5$) shows that the relative error in the interface length is always less than 10% and it is significantly lower for $\theta > 5°(\theta \to \pi/2)$ or for smaller and larger capillary numbers (Fig. 14b, for $a_v < 0.5$ and $a_v > 2$).

The conclusion that can be drawn in view of Figs. 11–14 is that the model of the constant characteristic curvature provides a good description of the phases geometry over the whole parameters space. Except for a small range of capillary numbers, $a_v \simeq 0.5$–1, and $\theta \to 0$ or $\theta \to \pi$, this model practically coincides with the exact solution.

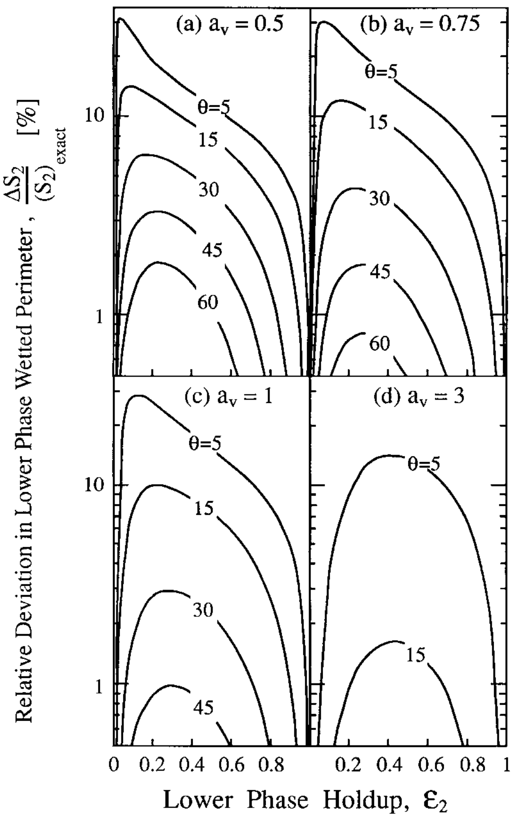

Fig. 13. The relative deviations in the values of the lower phase wetted perimeter associated with the model of constant characteristic curvature (Brauner et al., 1996b).

4. Discussion: implications to stratified flow solutions

The prediction of the location of the interface in two-phase stratified flow is necessary in order to obtain analytical or numerical solutions of the flow equations. Generally, the solution for the interface location is coupled with the solution of the flow equations, through the boundary conditions imposed on phases velocities and shear stresses components along the interface. However, in the particular case of fully developed unidirectional axial flow, the problem can be significantly alleviated by decoupling the solution for the interface location from the solution of the flow equations. For this case the solution for interface location is identical to that obtained in a static two-phase system with the same holdup. The governing equation, which determines the interfacial shape, can be derived either from the condition of equilibrium between the local pressure jump at the surface and local surface tension force, or by formulating the variational problem of minimizing the system total free energy. The energies which are subject to variation in this case are the potential energy in the gravitational field, the wall energy and interfacial energy.

It is of interest to note that for undeveloped axial flow, this variational problem is inconsistent with the flow equations and boundary conditions across the interface, since with

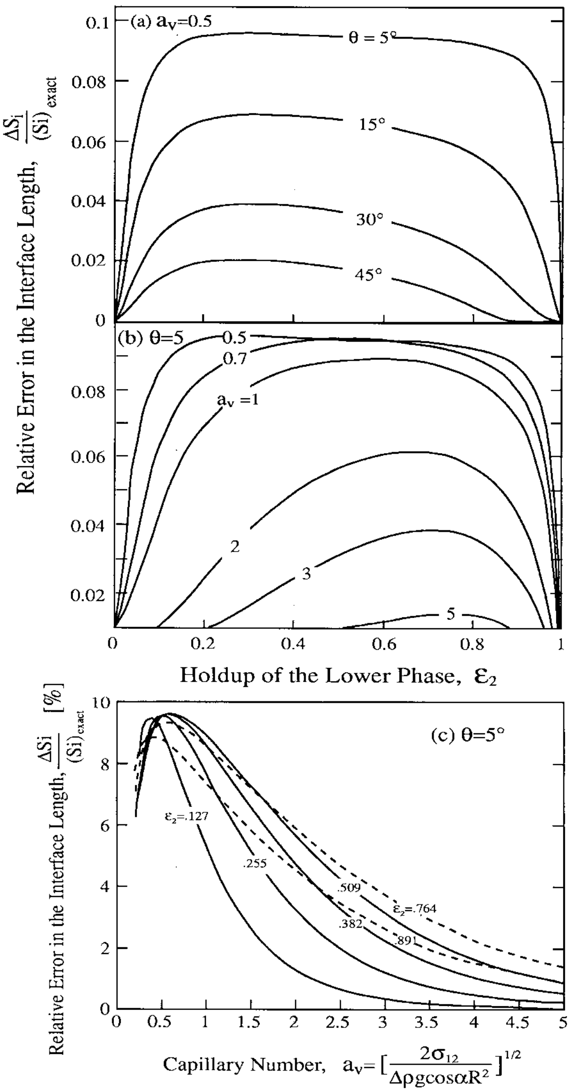

Fig. 14. The deviation in the interface length associated with the model of constant characteristic curvature (Brauner et al., 1996b).

$\partial u_1/\partial z, \partial u_2/\partial z \neq 0$, lateral velocity components must be non-zero. In this case, additional contribution to the energy (e.g., kinetic energies) may have to be accounted for, if a variational formulation can be justified at all. For a turbulent fully developed axial flow, the solutions obtained for the interfacial shape are applicable in case secondary flows and hydrodynamic shear stresses normal to the interface are negligible. It is worth emphasizing, however, that for high Reynolds number flow in systems of $a_v \simeq 1$ (or larger), the common assumption of a plane interface cannot be justified either, since gravity is no longer dominating. For sufficiently high Reynolds numbers (as encountered in the flow of a gas phase), lateral velocity components due to secondary flows and turbulent shear stresses (normal to the interface) may dominate the interface curvature.

In fully developed unidirectional axial flow, the location of the interface is determined by three non-dimensional parameters, which include the Eötvös number, $Eo = 2/a_v^2 = R^2 \Delta\rho g \cos a/\sigma_{12}$, the fluids/wall wettability angle, θ and the fluids holdup. The coupling with the hydrodynamic problem is through the fluids holdup, which should satisfy the momentum equations in the flow direction. In case of horizontal laminar flows, the flow equations add two dimensionless parameters: the fluids flow rates ratio, $\tilde{Q} = Q_1/Q_2$ and viscosities ratio, $\tilde{\mu} = \mu_1/\mu_2$ (Brauner et al., 1995), thus the dimension of the parameters space is increased to four. In inclined flow, and additional inclination parameter, $Y = \Delta\rho g \sin\alpha/(dP/dz)_{1s}$ evolves from the flow equations (Brauner et al., 1998), $(dP/dz)_{1s}$ is upper phase superficial pressure drop.

It is important to realize that capillary systems are not necessarily characterized by a small tube diameter. The analysis shows that diameter effects are incorporated in the non-dimensional Eötvös number and identical curved interfacial configuration will be obtained in large diameter tube (with low density differential, reduced gravity or inclined systems) of the same $Eo, \theta, \tilde{Q}, Y$ and $\tilde{\mu}$ as long as laminar flow prevails. Another important implication is the possibility of simulating two-phase flow under microgravity conditions by conducting terrestrial experiments. (For instance laminar gas–liquid flows in space can be simulated by liquid–liquid systems under normal gravity conditions, Brauner, 1990).

Analytical solutions of the flow equations can be obtained in case the curvature along the interface is constant. For such interfacial geometries the appropriate coordinate system is the bipolar coordinate system, which enables arriving at analytical expressions for the 2D profiles of the fluids axial velocity and shear stresses (Brauner et al., 1995, 1996a). In the limit of fully eccentric core-annular configuration, a special coordinate system is required (Rovinsky et al., 1997). Although the assumption of a constant curvature is rigorously valid only in the extremes of $a_v = 0$ or $a_v \to \infty$, this study identifies the ranges of parameters where this assumption can be justified. In practice, for $\theta \to 0$, or $\theta \to \pi$ the solutions of $a_v \to \infty$ can be applied already for $a_v > 10 = a_{vH}$ ($Eo < 0.01$) and the solution of a plane interface ($a_v = 0$) for $a_v < 0.1 = a_{vL}$ ($Eo > 100$). The value of a_{vH} decreases as the wetting tendency of the two fluids gets similar ($\theta \to \pi/2$) or with reducing the holdup of the non-wetting phase. On the other hand, for $\theta \neq 0$ and $\theta \neq \pi$, there is a particular value for the holdup where a plane interface exactly matches the wettability condition at the wall. For this particular holdup the system is pseudo gravity dominated, whereby the interface is plane irrespective of the capillary number ($a_{vL} \to \infty$).

The gap between a_{vL} and a_{vH} can be bridged by using the model for the characteristic curvature (Brauner et al., 1996b). The characteristic curvature corresponds to a curve of constant curvature, which yields the best approximation to the exact interfacial shape, since it satisfies the same variational principle of minimizing the system free energy. In fact, the approach used by Brauner et al. (1996b) is based on the well-recognized benefit of formulating differential equations as a variational problem, which then permits obtaining an approximate solution in terms of prescribed functions. Comparison of the exact solution with the corresponding characteristic curvature solution shows that the errors in describing the phases geometry are minimized over the entire parameters space. Thus, the characteristic curvature model suggests a possibility of obtaining analytical solutions which yield stratified flow characteristics over wide ranges of parameter values $Eo,\theta,\tilde{Q},Y$ and $\tilde{\mu}$. These analytical solutions were used to explore the significance of considering the interface curvature in predicting the pressure drop and holdup for a specified two-fluid system and operational conditions (Brauner et al., 1995).

The exact solution for the interface shape is of obvious importance when analytical solution of the flow equations cannot be obtained and the equations are solved numerically. Given Eo,θ and the holdup, the exact solution provides the interface location. Numerical schemes can be used to obtain the 2D axial velocity profiles for a given axial pressure drop and a gravity component. The corresponding fluids flow rates are then obtained by integrating the velocity profiles over the (known) fluids cross sectional area. The inverse problem, of obtaining a solution for the axial pressure drop and holdup for specified flow rates, generally requires an iterative procedure. The knowledge of the interface location under fully developed conditions is also of a major importance for setting an appropriate computational domain and analysis of the results of numerical simulations of 3D two-phase flows in a developing region, where the evolution of the interface from specified entry conditions is studied (see, for example, the numerical study by Ong et al., 1994 and the discussion in Brauner et al., 1996c).

The exact solution for the interface configuration can be also incorporated in simplified models for stratified flow, such as the two-fluid model. In this case, given Eo and θ, the geometrical variables (phases wetted perimeters, flow cross-sectional areas and the interface length) can be obtained in terms of an a-priori unknown location of the TP point, β (replacing the layer depth in case of a plane interface). When combined with the two-fluid momentum equations, a complete solution can be obtained for specified operational conditions (flow rates), which includes the pressure drop, holdup and the interfacial shape. More details are given in Gorelik (1999). The results are similar (practically identical) to that obtained by the two-fluid model for stratified flows with curved interfaces, recently presented by Brauner et al. (1998). The latter utilizes the characteristic (constant) curvature model for describing the interface. The deviations caused by the small inaccuracies in describing the exact interfacial shape are much less significant than other inherent inaccuracies and limitations of the two-fluid model (such as definitions of the hydraulic diameters and modeling of the wall and interfacial shear stresses (Gorelik, 1999; Brauner and Moalem Maron, 1989; Hall and Hewitt, 1993). The comparison of the two-fluid model predictions with experimental data of Valle and Kvandal (1995) for stratified oil–water flow ($a_v = 0.32$) was presented in Brauner et al. (1998). This comparison demonstrates the significance of accounting for the interfacial curvature in modeling stratified flows in liquid–liquid systems and other two-phase systems of a non-vanishing capillary number.

Another important result of the exact model is the expression obtained for the capillary pressure (Eqs. (21) and (30)) and its variation with the system parameters (Figs. 9 and 10). It is important to realize that for $0<\theta<\pi$, when neither of the phases ideally wets the tube wall, stratification in the system cannot be ruled out even in the limit of $a_v\rightarrow\infty$ (gravity is completely absent). In fact, the existence of stratified flow pattern in gas–liquid down flow through vertical capillaries was reported in the literature (Biswas and Greenfield, 1985). The capillary pressure is the key for analyzing the stability of stratified flow in systems of non-vanishing capillary number. In such systems the stabilizing (or destabilizing) forces evolve due to surface forces (surface tension and wall/fluids adhesion) and are manifested in variations of the capillary pressure with the interfacial shape and holdup in the presence of interfacial disturbances. On the other hand, the solution for the interfacial shape in systems of $a_v \gg 1$ and when one of the phases ideally wets the wall ($\theta = 0$ or π), shows that in such systems the fully eccentric core-annular configuration is the natural flow pattern, which can be obtained also in the limit of $Re \rightarrow 0$ in both phases. Indeed, core flow pattern in oil–water systems (where a highly viscous core is lubricated by an annular water film) is known to be promoted by minimizing the density difference between the fluids and using hydrophilic pipe material (Joseph and Renardy, 1992; Brauner, 1998). Obviously, stabilization of the core in a concentric position requires increasing the flow rates for evolution of stabilizing hydrodynamic forces which provide the necessary lift to balance the buoyancy force on the core.

5. Conclusion

The study addresses the problem of predicting the interface location in stratified flows. Analytical expressions are obtained for the interface shape and for the capillary pressure by solving the variational problem of minimizing the system free energy (potential and surface energies). It is shown that this variational principle is consistent with the hydrodynamic equations of unidirectional fully developed axial laminar two-phase flow in a conduit. Under these conditions, the solution is exact and is determined by three dimensionless variables: the holdup, fluid/wall wettability angle and the Eötvös number, $Eo = \Delta\rho g \cos\alpha R^2/\sigma_{12}$. The ranges of parameter values, for which either the model of flat interface ($Eo \rightarrow \infty$), or the model of constant curvature of $Eo = 0$ are applicable, are explored. It is also shown that the model of constant characteristic curvature (Brauner et al., 1996b) provides a good description of the interfacial shape and enables extending the parameters space where analytical solutions of stratified flow can be obtained.

Appendix A. The interface shape in a rectangular channel

Formulation of the variational problem for minimizing the system free energy of two fluids in a channel of a rectangular cross section (Fig. A1) leads to the following Euler–Lagrange (E-L) equation:

$$\tilde{\eta} + \Lambda - \frac{a_v^2}{2}\frac{\mathrm{d}}{\mathrm{d}\tilde{x}}\frac{\tilde{\eta}_{\tilde{x}}}{\sqrt{1+\tilde{\eta}_{\tilde{x}}^2}} = 0 \tag{A1}$$

where

$$a_v = \sqrt{\frac{2\sigma_{12}}{(\rho_1-\rho_1)g\cos\alpha W^2}};\quad \Lambda = \frac{\lambda}{(\rho_2-\rho_1)g\cos\alpha W} \tag{A2}$$

$$\tilde{x} = x/W;\quad \tilde{\eta} = \eta/W \tag{A3}$$

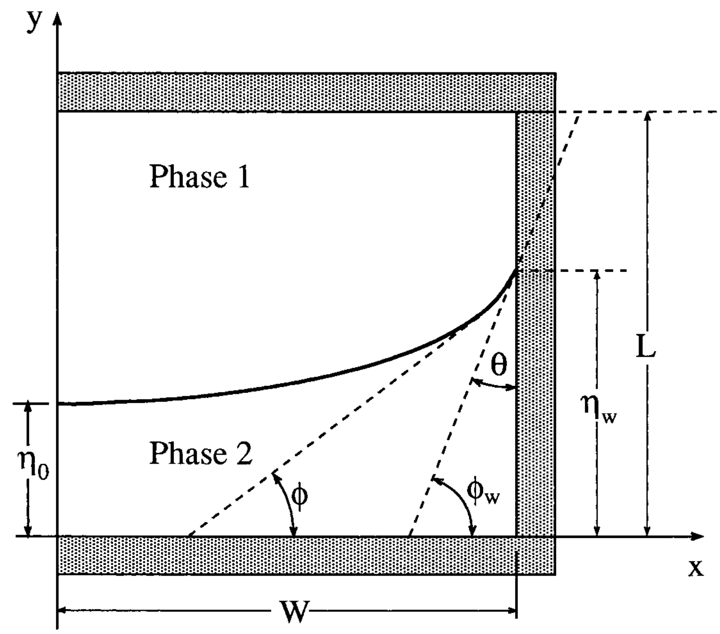

Fig. A1. Schematic description and coordinates in a rectangular cross section.

The natural boundary conditions are:

$$\tilde{x}=0;\quad \tilde{\eta}_{\tilde{x}}=0;\quad \phi=\pi$$

$$\tilde{x}=1;\quad \tilde{\eta}_{\tilde{x}}=\mathrm{ctg}\,\Theta;\quad \phi=\frac{\pi}{2}-\Theta \tag{A4}$$

where $\phi=tg^{-1}(\tilde{\eta}_{\tilde{x}})$. Note that here $\Theta<\pi/2$ corresponds to a wetting lower fluid. The constraint on the fluids volume is:

$$e_2=\int_0^1\tilde{\eta}\,\mathrm{d}\tilde{x}=\frac{V_2}{W^2}=\varepsilon_2\left(\frac{L}{W}\right) \tag{A5}$$

Integration of (A1) with respect to $\tilde{x}$ yields

$$\tilde{y}+\Lambda=\pm a_v\sqrt{A-\cos\phi} \tag{A6}$$

and

$$\mathrm{d}\tilde{x}=\mp\frac{a_v}{2}\frac{\cos\phi}{\sqrt{A-\cos\phi}}\mathrm{d}\phi \tag{A7}$$

where A is the integration constant. The upper sign in Eqs. (A5) and (A6) applies for $0\leq\Theta\leq\frac{\pi}{2}$ and the lower sign for $\frac{\pi}{2}\leq\Theta\leq\pi$. Utilizing the boundary condition at $\tilde{x}=0$ the solution of Eq. (A6) is:

$$\tilde{x} = \mp \frac{a_v}{2} \int_0^{\phi} \frac{\cos \phi}{\sqrt{A - \cos \phi}} \tag{A8}$$

The integral on the rhs of Eq. (A7) can be expressed in terms of elliptical integrals of the 1st and 2nd type. The solution for $x(\phi)$ is identical to that obtained in a circular cross section and is given by Eq. (17). Substituting boundary condition at $\tilde{x} = 1$ yields an implicit algebraic equation for A (or for $k = \sqrt{2/(A+1)}$):

$$\pm \frac{a_v k}{\sqrt{2}} \{ \left[\frac{2}{k^2} - 1 \right] \left[F_1\left(k, \frac{\pi}{2}\right) - F_1\left(k. \frac{\pi/2 + \Theta}{2}\right) \right] - \frac{2}{k^2} \left[F_2\left(k, \frac{\pi}{2}\right) - F_2\left(k, \frac{\pi/2 + \Theta}{2}\right) \right\} = 1 \tag{A9}$$

The value of the constant A approaches the value of 1 as $a_v \rightarrow 0$ and it increases with increasing a_v. For $a_v \gg 1$, a simple explicit expression can be obtained for A. Assuming $A \gg \cos \phi$, the integration in Eq. (A7) yields

$$A|_{a_v \rightarrow \infty} = A_\infty = \frac{a^2_v}{4} \cos^2 \Theta \tag{A10}$$

The approach of A to the asymptotic value given in Eq. (A9) is shown in Fig. A2. The capillary number where practically $A = A_\infty$ increases as the wettability angle approaches 90°. Obviously, for $\Theta = 90°$, the interface is flat, independently of the capillary number and $A = 1$. For high capillary numbers, the solution for the interface shape is given by:

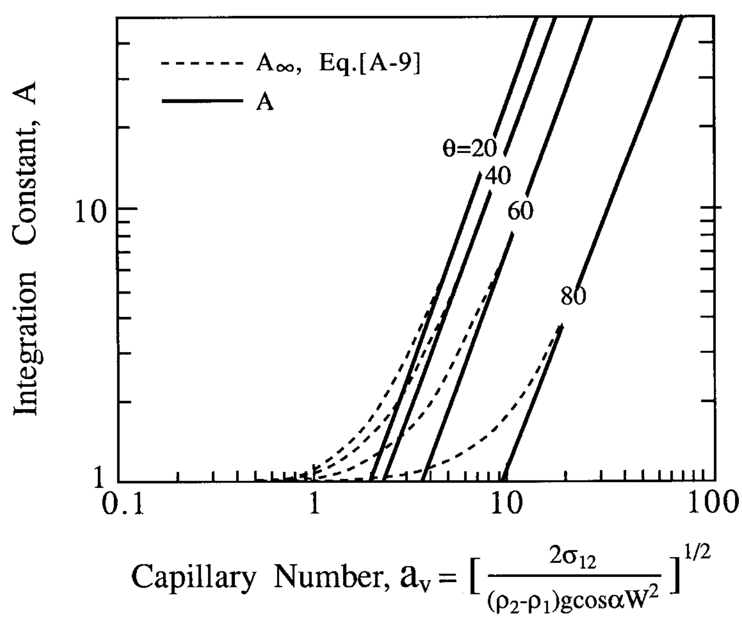

Fig. A2. Variation of the value of the integration constant, A with the capillary number and wettability angle.

$$\tilde{x} = \frac{a_v^2}{2\Lambda_\infty}\sin\phi$$

$$\tilde{y} = -\frac{a_v^2}{2\Lambda_\infty}\cos\phi + C$$

$$\tilde{\Lambda}_\infty = \frac{a_v^2}{2}\cos\Theta; \quad C = -\left[e_2 + \frac{1}{2}\right]\mathrm{ctg}\,\Theta \tag{A11}$$

It is to be noted that contrary to the solution in a circular conduit, the interface shape in a rectangular conduit (Eq. (17) with (A8)) is independent of the fluids holdup. The constraint on the fluids holdup affects only the average interface elevation from the bottom ($\eta = h = \varepsilon_2 L$) and the value of Λ. An equation for Λ can be obtained by integrating the terms in (A5) with respect to $\tilde{x}$ (in the limits $\tilde{x} = 0$ to $\tilde{x} = 1$) and utilizing Eq. (A4):

$$\Lambda = +\frac{a_v^2}{2}\cos\Theta - e_2 \tag{A12}$$

In the extreme of $a_v = 0$, the interface is plane and is given by $\tilde{\eta} = h/W = \varepsilon_2 L/W$ and Eq. (A1) yields:

$$\Lambda_0 = \Lambda|_{a_v=0} = -e_2 \tag{A13}$$

In this case, Λ is a constant dimensionless pressure along the interface and represents the 'floating' tendency of the lower phase. In the other extreme of $a_v \to \infty, \Lambda = \Lambda_\infty$ and is given in Eq. (A10).

Comparison of Eqs. (A10) and (A12) with Eq. (A11) shows that for the simple geometry under consideration the value of Λ is a superposition of the above two asymptotic values:

$$\Lambda = \Lambda_0 + \Lambda_\infty \tag{A14}$$

In fact, combining Eqs. (A1) and (A11) shows that for any a_v, the interface curvature at $\tilde{\eta} = \varepsilon_2 L/W$ (the point where the interface level attains the value corresponding to that obtained for a plane interface) is determined by the wettability angle:

$$-\frac{\partial}{\partial x}\frac{\eta_x}{\sqrt{1+\eta_x^2}}\bigg|_{\eta=h} = \frac{\cos\Theta}{W} \tag{A15}$$

and is identical to the (constant) interface curvature that would be obtained for $a_v \to \infty$. It is to be noted that for a finite a_v, the interface curvature at TP (contact point with the wall) is affected also by the hydrostatic pressure and is not given by Eq. (A14).

The above solution is valid in a bounded range of fluids holdup, where the solution for the interface shape is not constrained by the channel bottom, nor by the top wall. The bounds on the holdup can be calculated with reference to Fig. A3. When the lower fluid forms the more wetting phase, $0 \le \Theta \le \pi/2$, a lower bound on its holdup is obtained by considering the limiting situation where the lowest point touches the tube bottom. The additional boundary condition,

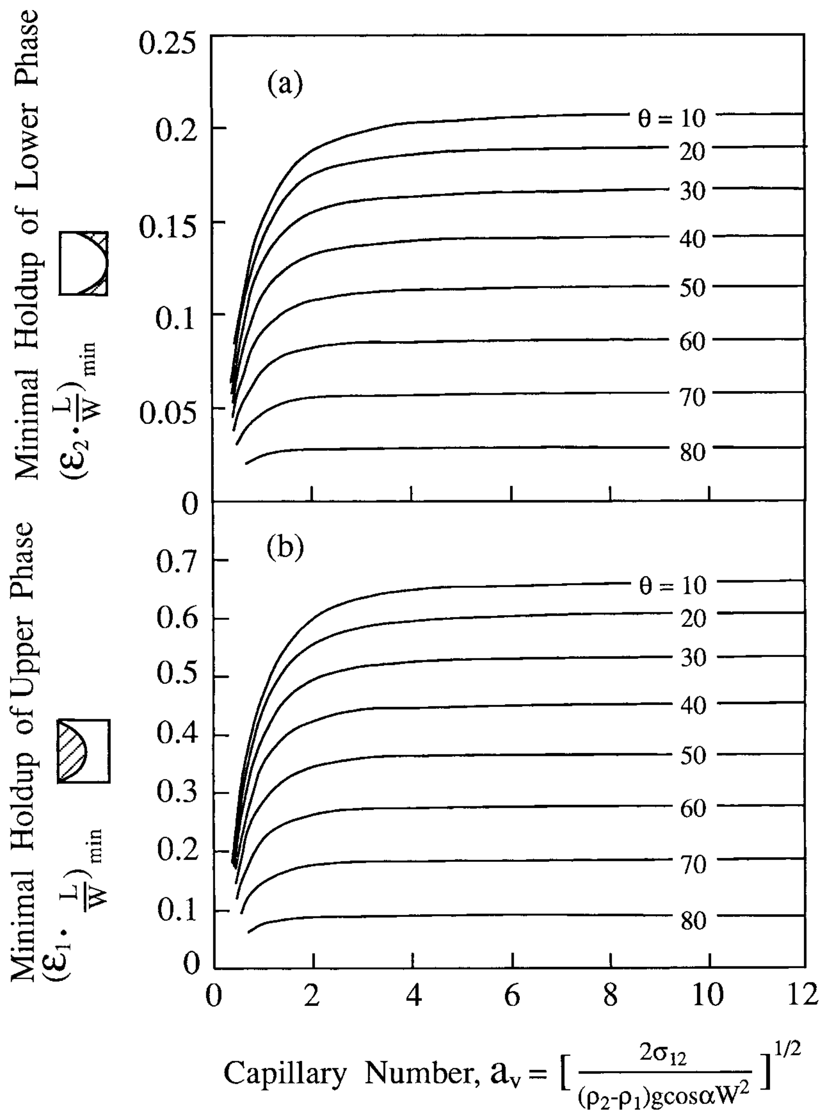

Fig. A3. Bounds on holdup for which the solution is valid—effect of a_v and Θ.

$y = 0$ at $x = 0$, permits calculation of $(e_2)_{min}$ corresponding to such configurations as function of the capillary number and wettability angle (Fig. A3a). When $a_v \gg 1,(e_2)_{min}$ approaches a constant value given by (Gorelik, 1999):

$$(e_2)_{min} = (\varepsilon_2 L/W)_{min} = \frac{1}{2\cos^2\theta}\left(\frac{\pi}{2} - \Theta\right) - \frac{1}{2}\text{ctg}\,\Theta \quad \text{for} \quad 0 \le \Theta < \frac{\pi}{2} \tag{A16}$$

For $\Theta = \pi/2,(e_2)_{min} \equiv 0$. Note that in case the upper fluid forms the wetting phase, $\frac{\pi}{2} < \Theta \le \pi$, Fig. A3a and Eq. (A15) gives the lower bound on $\varepsilon_1 L/W$ (or $(e_2)_{max}$)

An upper bound on ε_2 (for $0 \le \Theta < \pi/2$) is obtained by considering the situations where the interface climb on the side wall and reaches the top wall, $\tilde{\eta}_w = L/W$. Here too, the additional condition ($\tilde{\eta} = L/W$ at $\tilde{x} = 1$) yields the corresponding system holdup. The results as function of a_v and θ are given in Fig. A3b. The asymptotic values for $a_v \gg 1$ satisfies the following relation:

$$(e_2)_{\max} = 1 + \frac{1}{2}\mathrm{ctg}\,\Theta + \frac{1}{2\cos^2\Theta}\left(\frac{\pi}{2} - \Theta\right) - \frac{1}{\cos\Theta} \quad \text{for } 0 \le \Theta < \frac{\pi}{2} \tag{A17}$$

and $(e_2)_{\max} = 1$ for $\Theta = \pi/2$. For $\frac{\pi}{2} < \Theta \le \pi$ Fig. A3b and Eq. (A16) give the values of $(\varepsilon_1 L/W)_{\max}$ (or $(e_2)_{\min}$).

It is to be noted, however, that when the interface merge into the channel corner (see Fig. A3b), the wettability angle is practically undefined. If the wettability condition on the side wall is relaxed, a feasible solution for $0 \le \Theta < \pi/2$ and $e_2 > (e_2)_{\max}$ is that corresponding to any pseudo wettability angle $\Theta_p > \Theta$, which is unconstrained by the presence of the upper wall. The minimal Θ_p can be obtained from Fig. A3. Another possible solution for $e_2 > (e_2)_{\max}$ is that the lower fluid completely wets the side wall and partially the upper wall. Once the wettability angle on the upper wall is known, a solution for the interface shape can be obtained. The solution is, in principle, the same as that obtained for a 2D drop hanging from a horizontal support (Pitts, 1973). Valid solutions for the symmetrical case of $\frac{\pi}{2} < \Theta \le \pi$ and $e_2 < (e_2)_{\min}$ can be obtained in an analogue way.

For $0 \le \Theta < \pi/2$ and $e_2 < (e_2)_{\min}$, the constraint on the fluids holdup can be met only if the interface loses its continuity and the bottom wall dries out from the lower fluid over a length $2x_0$ around the channel center line. The unknown value of x_0 can be obtained via a solution which considers the fluid/bottom wettability angle, Θ_0. The case of $\Theta_0 = 0$ is of particular interest, as in most practical situation, the bottom is prewetted by the heavier fluid. In this case, the solution obtained for a continuous interface is valid, provided the characteristic length scale W (used for normalization) is replaced by $W(1 - \tilde{x}_0)$. Thus, given Θ (on the side wall), the corresponding curve on Fig. 3a provides a relationship between $\varepsilon_1 L/(W - x_0)$ and the pseudo capillary number, $a_{vp} = a_v/(1 - \tilde{x}_0)$ and can be used to extract $\tilde{x}_0$. The symmetrical situation of $\frac{\pi}{2} < \Theta \le \pi$ and $e_2 > (e_2)_{\max}$ can be treated in a similar way.

The above limitations on the fluids holdup may not be of practical significance if surface tension effects are due to a narrow channel (and L/W is large). However, when $a_v \gg 1$ is due to vanishing $\Delta\rho$ or $g\cos\alpha$, these bounds should be considered.

References

Abramowitz, M., Stegun, I.A., 1964. Handbook of Mathematical Functions with Formulas, Graphs and Mathematical Tables. United States Department of Commerce, Washington, D.C.

Bentwich, M., 1964. Two-phase axial flow in pipe. Trans. ASME, Series D 86 (4), 669–672.

Bentwich, M., 1976. Two-phase laminar flow in a pipe with naturally curved interface. Chem. Eng. Sci. 31, 71–76.

Biswas, J., Greenfield, P.F., 1985. Two-phase flow through verticle capillaries-existence of a stratified flow pattern. Int. J. Multiphase Flow 11 (4), 553–563.

Brauner, N., 1990. On the relations between two-phase flows under reduced gravity and earth experiments. Comm. Heat and Mass Transfer 17 (3), 271–281.

Brauner, N., 1998. Liquid–Liquid two-phase flow. In: Schlunder E.U., Hewitt G.F. (Eds.), HEDH/HEDU, Heat Exchange Design Handbook.
Brauner, N., Moalem Maron, D., 1989. Two-phase liquid–liquid stratified flow. Physico-Chem. Hrdrodynam. 11, 487–506.
Brauner, N., Rovinsky, J., Moalem Maron, D., 1995. Analytical solution of laminar stratified flow with curved interfaces. In: Proceedings of the NURETH-7 Meeting ANS, vol. 1, 192–211.
Brauner, N., Rovinsky, J., Moalem Maron, D., 1996a. Analytical solution for Laminar–Laminar two-phase flow in circular conduits. Chem. Eng. Comm. A 141/142, 103–143 (Dukler Memorial Issue).
Brauner, N., Rovinsky, J., Moalem Maron, D., 1996b. Determination of the interface curvature in stratified two-phase systems by energy considerations. Int. J. Multiphase Flow 22, 1167–1185.
Brauner, N., Rovinsky, J., Moalem Maron, D., 1996c. Characteristics of annular and stratified two-phase flows in the limit of fully eccentric annular configuration. In: Proc. of ExHFT 4, Brussels, June 2–6, vol. 2, 1189–1204.
Brauner, N., Moalem Moran, D., Rovinsky, J., 1998. A two-fluid model for stratified flows with curved interfaces. Int. J. Multiphase Flow 24, 975–1004.
Gorelik, D., 1999. Interface shape between two immiscible layers and its effect on the flow characteristics. M.Sc. thesis, Faculty of Engineering, Tel Aviv University.
Grandsteyn, I.S., Rezhik, I.M., 1980. In: Jeffrey, A. (Ed.), Tables of Integral, Series and Products. Academic Press, New York.
Hall, A.R., Hewitt, G.F., 1993. Application of two-fluid analysis to laminar stratified oil–water flows. Int. J. Multiphase Flow 19 (4), 711–717.
Joseph, D.D., Renardy, Y., 1992. Fundamentals of Two-Fluid Dynamics. Springer–Verlag, New York.
Masliyah, J.H., Shook, C.A., 1978. Two-phase laminar zero net flow in circular inclined pipe. Can. J. Chem. Eng. 56, 165–175.
Moalem Maron, D., Rovinsky, J., Brauner, N., 1995. Analytical prediction of the interface curvature and its effects on stratified flow characteristics. In: Celata, G.P., Shah, R.K. (Eds.), Proc. of the Int. Symp. on two-phase flow modeling and experimentation, vol. 1. Edizioni ETS, pp. 163–170.
Ong, J., Enden, G., Popel, A.S., 1994. Converging three dimensional Stokes flow of two fluids in a T-type bifurcation. J. Fluid Mech. 270, 51–71.
Pitts, E., 1973. The stability of pendent liquid drops. Part 1: Drops formed in a narrow gap formed in a narrow gap. J. Fluid Mech. 59 (4), 753–767.
Ranger, K.B., Davis, A.M.J., 1979. Steady pressure driven two-phase stratified laminar flow through a pipe. Can. J. of Chem. Eng. 57, 688–691.
Rovinsky, J., Brauner, N., Moalem Maron, D., 1997. Analytical solution for laminar two-phase flow in a fully eccentric core annular configuration. Int. J. Multiphase Flow 23, 523–542.
Semenov, N.L., Tochigin, A.A., 1962. An analytical study of the separate laminar flow of a two-phase mixture in inclined pipes. J. Eng. Phys. 4, 29.
Valle, A., Kvandal, H.K., 1995. Pressure drop and dispersion characteristics of separated oil–water flow. In: Celata, G.P., Shah, R.K. (Eds.), Proc. Int. Symp. on two-phase flow modeling and experimentation, Oct. 9–11, Rome, Italy, vol. 1. Edizioni ETS, pp. 583–591.